Investigating Spatio-Temporal Cellular Interactions in Embryonic Morphogenesis by 4D Nucleus Tracking and Systematic Comparative Analysis — Taking Nematodes *C. elegans* and *C. briggsae* as Examples

Guoye Guan
Center for Quantitative Biology
Peking University
Beijing, China
guanguoye@gmail.com

Ming-Kin Wong
Department of Biology
Hong Kong Baptist University
Hong Kong, China
16484142@life.hkbu.edu.hk

Lu-Yan Chan
Department of Biology
Hong Kong Baptist University
Hong Kong, China
16483669@life.hkbu.edu.hk

Vincy Wing Sze Ho
Department of Biology
Hong Kong Baptist University
Hong Kong, China
vincy.wsh@gmail.com

Xiaomeng An
Department of Biology
Hong Kong Baptist University
Hong Kong, China
anxm@hku-szh.org

Zhongying Zhao
Department of Biology
State Key Laboratory of Environmental and Biological Analysis
Hong Kong Baptist University
Hong Kong, China
zyzhao@hkbu.edu.hk

Chao Tang
Center for Quantitative Biology
Peking-Tsinghua Center for Life Sciences
School of Physics
Peking University
Beijing, China
tangc@pku.edu.cn

2021 IEEE 9th International Conference on Bioinformatics and Computational Biology (ICBCB) | 978-1-6654-1500-2/21/$31.00 ©2021 IEEE | DOI: 10.1109/ICBCB52223.2021.9459206

***Abstract*—Metazoan embryonic morphogenesis is involved with spatio-temporal interactions between cells during embryogenesis from zygote to larva. These regulatory interactions (e.g. active and passive cell motion driven by cytomechanics) contribute to precise, robust and stereotypic embryo patterns among individuals of a species. To in-depth decipher the underlying mechanism and biological function of such interactions, in this work, we used two closely related species *Caenorhabditis elegans* and *Caenorhabditis briggsae* as examples and provided a general framework for system-level comparative analysis. We cultured and imaged 11 wild-type embryos *in vivo* using 3-dimensional time-lapse confocal microscope for each species, with following automatic nucleus-based cell tracking. We quantitatively constructed their normalized and comparable 4D cell-position atlas *in silico*, including information like each cell's division timing and migration trajectory during embryogenesis from 4- to 350-cell stage. With highly similar cell lineage in both *C. elegans* and *C. briggsae*, we compared their division-timing program and cell-arrangement pattern globally and locally, which revealed a turning point of regulation on positional variation among individuals, within one species as well as between two species. Moreover, this down regulation could rescue some cellular positional variation caused by division-order chaos between *C. elegans* and *C. briggsae*. Last but not least, the asynchrony of division between sister cells were found to be functional for local positioning of the newborn cells. Our information-rich dataset and the computational analytic methods could facilitate related research in developmental biology, evolutionary biology, and comparative biology.**

Keywords—embryonic morphogenesis, spatio-temporal cellular interaction, nucleus tracking, comparative analysis, nematode, C. elegans, C. briggsae

I. INTRODUCTION

The 3-dimensional multicellular system evolves over time during metazoan embryo development with high accuracy regarding both space and time [1, 2]. These stereotypic embryonic patterns are comprised of cell number, cell position, cell division timing, cell division orientation, cell fate, transcriptome, proteome, and so forth, which are critical to a number of significant biological events such as cell-cell signaling transduction and tissue formation [3-5], and determine the anatomy of a species [6, 7]. Importantly, the interrelationship between cell division timing and cell position as well as their consequent side effects and chain effects (e.g. cell-cell contact relationship and area), were recently proposed to play a pivotal role in development at the mechanical and kinematic level [8-10], and are conclusively referred to as "spatio-temporal cellular interactions in embryonic morphogenesis" in this paper.

Caenorhabditis elegans (i.e. *C. elegans*), classified as "eutelic" animal (e.g. rotifer, nematode, gastrotrich) which has a constant total number of somatic cells in adult [11], has been widely used in developmental biology research due to its conserved developmental programs among individuals at cellular level; in other words, each cell during embryogenesis has repeatable, identifiable and unique behavior as well as function [1, 2, 12]. Compared to other animals such as fly, frog, zebrafish and mouse, the transparent nematode not only has much smaller body size and less cell number, but also maintains plenty of cell types (e.g. muscle, neuron, pharynx), making it a popular model organism. Besides, the highly stereotypic and reproducible cellular behaviors during nematode development are also natural and useful materials for

study on the problem "spatio-temporal cellular interactions in embryonic morphogenesis". An explicit example of such problem is that, under control of basic mechanical laws, how cell divisions are coordinated spatially and temporally (i.e. division orientation and timing) to ensure the precision and robustness during embryo development [8].

Using *C. elegans* as model system, a lot of researches have been carried out to uncover the mechanisms of accurate and directional embryonic morphogenesis, from both perspectives of intercellular biophysics and intracellular biochemistry. With physical modeling and simulation, Fickentscher et al. (2013, 2016, 2018) proposed that the cell movements before gastrulation onset (~26-cell stage) can be simulated by cell-cell repulsion and volume-dependent clocks for cell division [9, 13, 14]. Kajita et al. (2002, 2003) and Yamamoto et al. (2017) elucidated the conditions required for correct formation of 4-cell arrangement pattern, and explained the key functions of asymmetric adhesion and eggshell shape in guiding appropriate cell packing [15-17]. Tian et al. (2020) and Kuang et al. (2020) theoretically demonstrated that both cell division orientation and timing dominantly affect the evolution of embryo structure [8, 10]. On the other hand, many active regulations on cell migration continue to be reported, for instance, the ingression of gut precursor cells E2 is mainly driven by actomyosin contractility and asymmetric adhesion [18, 19]. Besides, a cell's division orientation can be modulated by multiple mechanisms on the basis of cell-cell physical contact and directional cortical myosin flow [20, 21].

Even though all kinds of artificial perturbation (e.g. RNA interference, laser ablation, eggshell removal, external compression) and subsequent comparative analysis with wild-type embryo have been applied to *C. elegans* embryogenesis research [22-25], those operations sometimes cause pleiotropic defects and induce numerous potential influence factors, possibly making the conclusions obtained from comparative analysis less convincing [2, 26]. To overcome this shortcoming, some closely related nematode species have been introduced (e.g. *Halicephalobus gingivalis*, *Romanomermis culicivorax*), for that these systems have similar developmental programs and ability to hatch normally, meanwhile with different level of distinguishable characteristics which can be used for comparative research on embryo morphology as well as spatio-temporal cellular interactions [27-35].

Caenorhabditis briggsae (i.e. *C. briggsae*), one of the most closely related species to *C. elegans* [36], has been introduced into comparative research along with *C. elegans* and other similar nematode species, revealing a highly conserved spatio-temporal developmental procedure including both cell division timing and cell arrangement pattern [37, 38], in spite of their divergence in genome [39-41]. Nevertheless, a few significant and distinguishable differences on embryo morphology between *C. elegans* and *C. briggsae* have been quantitatively identified. Furthermore, those differences in cell division timing and cell arrangement pattern were found to be correlated, suggesting that these two species could be valuable and comparable materials for research on spatio-temporal cellular interactions in embryonic morphogenesis [37]. However, a more reliable dataset for comparative analysis should include abundant embryo samples (e.g. sample size > 10) with same level of quality control as well as recorded duration long enough (e.g. 4- to 350-cell stage for *C. elegans* and *C. briggsae*), which still needs to be collected and established.

Thanks to the progress and advance in 3D time-lapse *in vivo* imaging technique (e.g. confocal microscope) as well as automatic software for cell recognition, tracing and lineaging (e.g. StarryNite, AceTree) [42-44], division and migration of each cell during nematode embryogenesis can be captured experimentally and simultaneously at second- to minute-level resolution, with high efficiency and integrity and low error rate. These tools used fluorescently-labeled cell nucleus to represent the central location of a cell, so as to facilitate systematic observation and analysis on the morphogenesis of a whole embryo with all cells tracked simultaneously. Thus, they accelerated the high-quantity information collection of nematode embryonic morphogenesis in both wild-type and mutant of different species, producing 4D quantitative cell-position data of thousands of embryos, which is worth of deep mining with systematic computational methods [2, 37, 38, 45]. As a result, researchers can conveniently culture and image a whole nematode embryo with subsequent nucleus-based cell tracking, which consequently generates its complete atlas of embryogenesis and morphogenesis (e.g. cell identity, position, division orientation and timing) for further biological research.

In this work, we proposed a general and applicable framework for cross-species comparative analysis on embryogenesis and morphogenesis. Using nematode species *C. elegans* and *C. briggsae* as examples, we first cultured and imaged 11 wild-type embryos for each from 4- to 350-cell stage, quantitatively and statistically generating a 3D time-lapse dataset of cell-nucleus position. After linear normalization to minimize global variation among individuals, both sets of embryo structures were compared to each other globally and locally. Meanwhile, changes of division order between cell groups as well as their subsequent spatial effects were also analyzed. The correlation between cell division timing and cell arrangement pattern was inspected in detail with several special cases, including the recovery of positional variation between two nematode species as well as the asynchrony of division between sister cells.

II. Establishment of Two Comparable Systems

A work flow for generating comparable multicellular systems is summarized below (Fig. 1). Note that the biological system discussed in this paper consists of 3D time-lapse data of division and migration for every cell inside a live nematode embryo. Apart, we will utilize *C. elegans* and *C. briggsae* as examples and for illustration.

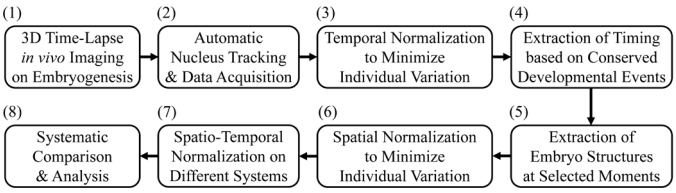

Fig. 1. Work flow of quantitative and comparative analysis on 4-dimensional spatio-temporal data between different multicellular systems, including eight key steps.

A. *Acquisition of 4D Cell-Position Data*

Embryos from different species should be cultured under respectively optimal environments and then imaged within the same time range defined by developmental stage, using 4D microscopic techniques. Position of each cell must be quantitatively captured from raw images and forms a complete dataset to describe the whole morphogenetic procedure at single-cell level. Manual editing is usually required to further confirm that the nucleus tracking for both cell identity and position is correct. Moreover, the identical cells in each embryo sample should be recorded with same or similar lifespan, so as to establish comparable data with equivalent standard and little bias.

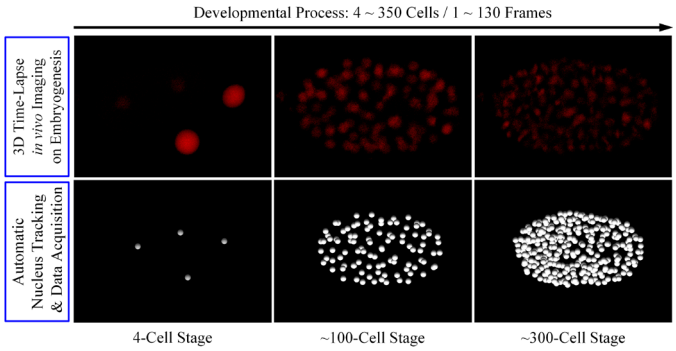

Fig. 2. *In vivo* experiment and quantitative data acquisition of cell position from 4- to 350-cell stage, using *C. briggsae* embryo with mCherry marker expressed and localized in nucleus for illustration.

Here, we collected 11 wild-type embryos of *C. elegans* (strain RW10481 [46]) and *C. briggsae* (strain *stIs*20027 [47]) respectively, which constantly expressed distinguishable fluorescent marker on each and every cell's nucleus. Then we performed *in vivo* imaging from 4- to 350-cell stage (~550 cells in hatching larva) along with following automatic nucleus-based cell tracking and manual quality-control editing (Fig. 2), producing 4D data of all the cells with complete lifespans recorded (Fig. 3), including AB4-AB128 (6 generations), MS1-MS16 (5 generations), E1-E8 (4 generations), C1-C8 (4 generations), D1-D4 (3 generations), P3 and P4. All those cells' daughters, namely AB256, MS32, E16, C16, D8, Z2 and Z3 (daughters of P4 which remain undivided [1]), were confirmed to be recorded with their initial appearance. Moreover, the first valid time point was set to be the last moment of 4-cell stage, which means that information of the four primary founder cells ABa, ABp, EMS and P2 were incomplete and not considered until the synchronous divisions of AB2 [2]. It's worth pointing out that, the cell name is given according to the founder cell it comes from (prefix) and its location relative to its sister's (suffix), which makes each cell identifiable and trackable [1]. For the 4D cell-position data we provided here, temporal resolution was set to be 1.41 or 1.54 min/frame, while spatial resolution was set to be 0.09 μm/pixel in focal plane (anterior-posterior axis and dorsal-ventral axis) and 0.71 or 1.01 μm/pixel perpendicular to the focal plane (left-right axis) (Table 1).

TABLE I. INFORMATION OF COLLECTED EMBRYO SAMPLES

Serial Number of Embryo Sample [s]	Time Resolution (min / frame)	Left -Right Resolution (μm / pixel)	Terminal Cell Number	Total Frame Number
e1	1.54	1.01	376	133
e2	1.54	1.01	379	135
e3	1.41	0.71	362	137
e4	1.41	0.71	361	138
e5	1.41	0.71	363	135
e6	1.41	0.71	362	132
e7	1.41	0.71	363	138
e8	1.41	0.71	366	134
e9	1.41	0.71	361	137
e10	1.41	0.71	361	135
e11	1.41	0.71	363	134
b1	1.41	0.71	383	151
b2	1.41	0.71	428	154
b3	1.41	0.71	371	143
b4	1.41	0.71	394	152
b5	1.41	0.71	378	144
b6	1.41	0.71	383	149
b7	1.41	0.71	369	148
b8	1.41	0.71	560	182
b9	1.41	0.71	384	145
b10	1.41	0.71	364	142
b11	1.41	0.71	375	147

s. prefix "e" for *C. elegans* and "b" for *C. briggsae*.

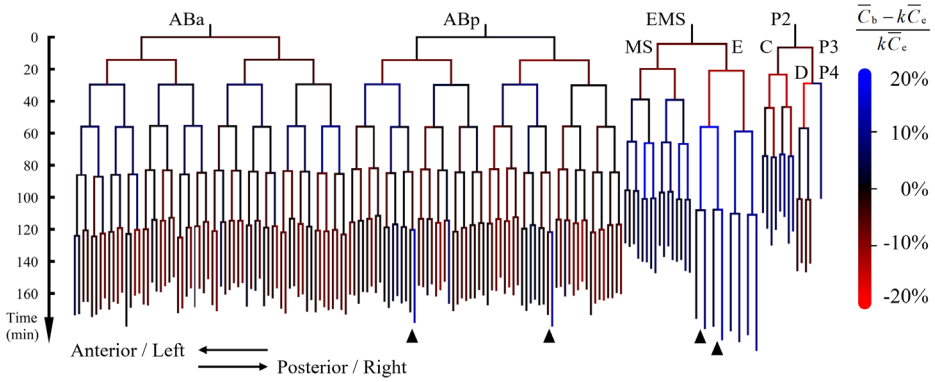

Fig. 3. Cell lineage tree of *C. briggsae* from 4- to 350-cell stage. All the cells with complete lifespan recorded are plotted as branches, with length corresponding to their average cell cycle respectively; different color represents the relative deviation of cell cycle from *C. elegans* to *C. briggsae*, according to (1); four pairs of cells with extra ADS in *C. briggsae* but not in *C. elegans* are indicated with black triangles; *k* denotes the ratio of global growth rate between the two species.

Consequently, we obtained a 3D time-lapse cell-position dataset $\{\boldsymbol{r}_{s,n,i,j}\}$. s, selected species (s = "e" for *C. elegans* and "b" for *C. briggsae*); n, serial number of embryo sample (n = 1 ~ 11 in this work); i, imaging time point (i.e. frame; $i \approx 1 \sim 130$ in this work); j, identity of specific cell (e.g. j = "EMS" for the EMS cell); $\boldsymbol{r}$, position of cell j at time point i, in embryo sample n of selected species s (Table 1).

B. Timing Selection based on Conserved Developmental Events

Intrinsic variation always exists in division timing and order of cells, for instance, division orders among cells within a synchronous-dividing group like AB2, AB4 and AB8 are extremely random, making the absolute timing of their daughters' appearance close to each other but vary from embryo to embryo (Fig. 3) [2]. Hence, to get over this temporal noise on cell list, developmental landmarks such as gastrulation activation and production of founder cells can be used as appropriate check time for reliable comparison between closely related species [2, 27, 28, 35].

As *C. elegans* and *C. briggsae* have highly common cell division pattern, which is comprised of several tissue-specific founder cells (e.g. AB, MS, E, C, D) with rounds of synchronous divisions respectively, we chose these division events as inspection time for that they are always shared among embryos of both species (Fig. 3) [37]. For each cell group that divide synchronously, the first and last co-existence moment of cells were taken into account as two distinct inspection timings respectively, establishing a temporal series consisting of 54 moments (27 division events) in each embryo sample of both species. Therefore, the cell-position dataset could be expressed in $\{\boldsymbol{r}_{s,n,i',j}\}$ after replacing i with i', where i' represents the inspection timing defined by developmental events conserved between individuals and between species (i' = 1 ~ 54 in this work) [48].

C. Minimization of Global Variation among Individuals

Due to unavoidable internal noise (e.g. thermal motion) and external noise (e.g. slide compression) during embryogenesis, global variation including cell division timing and cell position usually exists among individuals, which influences the absolute value of data but has little effect on the relative information such as division order and structure topology.

To minimize this global variation, proportionally linear normalization based on cell cycle within *C. elegans* as well as *C. briggsae* embryos was performed respectively. After that, each embryo within a species would acquire the same global growth rate. Next, for each species, spatial normalization including rotation, translation and scaling was carried out onto all the embryos consecutively and alternately, outputting a set of uniform multicellular structures with minimal variation and extremely close to each other. These two noise-elimination procedures have been tested and demonstrated in our previous works [2, 48].

D. Minimization of Global Variation between Species

After obtaining the normalized and standard 4D cell-position data of each species, further normalization on space and time needs to be executed between the two groups of embryo samples, to minimize their global variation and make them more comparable with respect to both cell division timing and cell position.

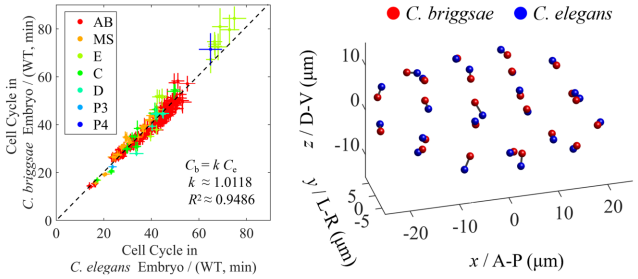

(a) (b)

Fig. 4. Global linear normalization between embryo groups of *C. elegans* and *C. briggsae*, including (a) cell cycle (MEAN ± STD); (b) cell position (MEAN), illustrated with the 24-cell stage here.

The normalization operations for two species are like the ones for samples within one species [2, 48]. After time normalization, both *C. elegans* and *C. briggsae* have the same global growth rate, while the original cell cycles exhibit a ratio between them as $k = 1.0118$ ($C_b \approx k \cdot C_e$, C_e for cell cycle in *C. elegans*, C_b for cell cycle in *C. briggsae*), indicating that *C. elegans* grows a little bit faster than *C. briggsae* in the experimental environment. The relative deviation of each cell from *C. elegans* to *C. briggsae* is defined as (1) (Fig. 3, Fig. 4a).

$$V = \frac{\overline{C}_b - k\overline{C}_e}{k\overline{C}_e} \tag{1}$$

On the other hand, cell positions from both species were very close to each other after space normalization, with different level of spatial shift as their statistical difference (Fig. 4b). For a targeted cell j at a selected inspection time i', this deviation is quantified by positional variation η, namely the distance between the cell's average positions in those two species, according to (2).

$$\eta_{i',j} = \left| \overline{\boldsymbol{r}}_{b,i',j} - \overline{\boldsymbol{r}}_{e,i',j} \right| \tag{2}$$

Similarly, at the selected inspection time i', global spatial deviation can also be calculated using the *C. elegans* embryo pattern as reference, as shown in (3).

$$\overline{\eta}_{s,i'} = \frac{1}{N_n} \sum_{n} \sum_{j'} \frac{\left| \boldsymbol{r}_{s,n,i',j'} - \overline{\boldsymbol{r}}_{e,i',j'} \right|}{N_{j'}} \tag{3}$$

Here, j' denotes the cells which appear in all the embryos involved, and $N_{j'}$ denotes the count of these unidentical cells; N_n denotes the sample number of the selected species (N_n = 11 in this work); the global positional variation calculated represents the mean shift of a cell from *C. elegans* average reference to the selected embryo samples. When s = "e", it represents the endogenous positional variability within *C. elegans* individuals [45]. When s = "b", it represents the positional variation between *C. elegans* and *C. briggsae*. It should be pointing out that, regarding the cell lists respectively conserved in *C. elegans* and *C. briggsae*, if the difference of

cell number between them reaches 10% of the cell number in *C. elegans*, the selected inspection moment would be omitted as incomparable outlier because of the disparate cell list.

So far, we have established a quantitative and comparable 4D cell-position system with *C. elegans* and *C. briggsae* embryos, including 11 samples from each species for statistics. Next, we will analyze this system at both global and local scales using a couple of cases, and then address its value to the research on spatio-temporal cellular interactions in embryonic morphogenesis.

III. Global Difference Between Species

We first investigated the global deviation in the aspects of cell division order and cell position, and probed into their interactions. In this section, we would use *C. elegans* as reference and see the natural perturbation or difference raised in *C. briggsae*. Among the 27 synchronous division events, in all, there are 8 division orders between them substantially changed, which are conserved with frequency over 90% among embryo samples in *C. elegans* but lower than that in *C. briggsae* (Table 2). Note that the division-order screening on *C. elegans* here was performed using another set of temporal data from our previous work (222 embryos in total), considering its much more adequate sample size for identifying the conserved cell division orders [2].

TABLE II. Difference of Cell Division Order

	Cell Group A	Cell Group B	Frequency of ($t_A \geq t_B$) in *C. elegans* (%) [R, A, B]	Frequency of ($t_A \geq t_B$) in *C. briggsae* (%) [R, A, B]
1	AB64	P4	99.6 (221/222)	81.8 (9/11) [c]
2	AB128	MS16	99.1 (220/222)	72.7 (8/11) [#]
3	E2	AB16	97.3 (216/222)	54.6 (6/11) [a]
4	E4	P4	93.7 (208/222)	81.8 (9/11) [c]
5	C8	P4	99.1 (220/222)	81.8 (9/11) [c]
6	D1	AB16	100.0 (222/222)	81.8 (9/11) [a]
7	D2	MS8	100.0 (222/222)	45.5 (5/11) [b]
8	D2	P4	99.1 (220/222)	63.6 (7/11) [b,c]

R. data obtained from Reference [2] (Guan, et al. 2019).
A. t_A denotes the division timing of the first dividing cell in Cell Group A.
B. t_B denotes the division timing of the last dividing cell in Cell Group B.
#. the last round of complete and synchronous cell divisions recorded.
a. perturbation on AB16, E2 and D1.
b. perturbation on D2.
c. perturbation on P4.

Division-order change between AB128 and MS16 was not further studied, for the reason that they're both the last round of complete cell divisions recorded (i.e. AB128 → AB256, MS16 → MS32) and have little follow-up data. Notably, the left changes can be summarized into 3 characteristic groups (Table 2). The first is divisions of AB16, E2 and D1, which all occur in a very short interval. The second is perturbation on D2 divisions (i.e. D2 ~ MS8, D2 ~ P4) while the third is perturbation on P4 (i.e. E4 ~ P4, C8 ~ P4, D2 ~ P4). Next, we'll look deep into these 3 groups and explore how division-order chaos disturb embryonic morphogenesis.

A. A Turning Point of Positional Variation within One Species as well as between Two Species

All the divisions of AB16, E2 and D1 occur in a very short time window (approximately 12 minutes in *C. elegans* and 6 minutes in *C. briggsae*), when the total cell number inside embryo is about 28 (Fig. 5a). Intriguingly, this timing is around the robust onset of maternal-zygotic transition and gastrulation [18, 19, 49], when intestinal precursor cells E2 start to ingress actively. Before these 3 division events, the division orders maintain conserved and invariant in both species (P0 → AB → P1 → AB2 → EMS → P2 → AB4 → MS&E → C → AB8&P3 → MS2 → C2) [2, 28]. Several mechanical models previously proposed for the development prior to gastrulation proved that accurately regulated cell division timing is necessary for proper cell migration [8-10]. However, the upcoming disorder in these 3 division events between *C. elegans* and *C. briggsae* implied that extra regulation may be crucially activated to guide the later morphogenesis, allowing the whole system's migratory movement to rely less on the strictly-controlled proliferation paces and division orders of cells, as well as the relaxation process passively coordinated via intercellular repulsion-attraction force [8-10, 13-17].

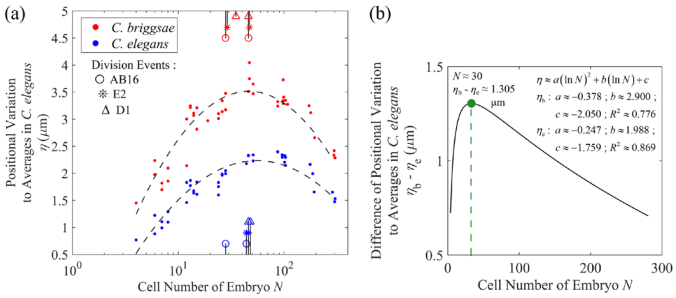

Fig. 5. Global positional variation to the averages of *C. elegans* embryos, according to (3). (a) Variation (variability) within *C. elegans* (η_e) is plotted with blue dots, while variation between *C. elegans* and *C. briggsae* (η_b) is plotted with red dots; both initial and terminal timings of AB16, E2 and D1 divisions are illustrated with colored circle, asterisk and triangle respectively; (b) difference of global positional variation between *C. elegans* and *C. briggsae* (η_b - η_e) is calculated and illustrated using the fitted curves of both species, with a sharp peak when cell number roughly reaches 30.

All the embryo samples from both species were compared to the averages of cell position in *C. elegans* reference, so as to show the global positional variation within one species as well as between two species (Fig. 5a). The global positional variation (variability) within *C. elegans* embryo samples obeyed a "low-high-low" dynamics, which was recently reported to be controlled by cell fate specification as well as cell adhesion and gap junction [45]. The turning point (i.e. start of plateau from 30- to 100-cell stage) is exactly around the first changes of division orders, namely, the orders of cell divisions of AB16, E2 and D1. Strikingly, similar pattern also existed in comparison between *C. elegans* and *C. briggsae*. The variation of *C. briggsae* is larger than that of *C. elegans*, indicating the slight but significant difference between them, even though their morphologies appear highly identical to naked eyes (Fig. 4b) [37, 38]. The difference of variation between them also reached a peak around these division timings (maximum difference η_b - $\eta_e \approx 1.305$ μm, cell number ≈ 30, cell radius ≈

5.3 ± 0.4 μm) (Fig. 5b) [48] In a word, the global positional variation between two species increased over time at first and then outstandingly started to decrease, probably regulated by the same underlying mechanisms [45]. Despite all this, global difference of cell position would consistently exist between *C. elegans* and *C. briggsae* embryos.

B. Regulatory Recovery of Positional Variation Caused by Change of Division Orders

In the case of another two sets of cells (i.e. D2 and P4), which consist of a small amount of cells and have division-order changes with at least two other cell groups respectively, cellular positional variation between *C. elegans* and *C. briggsae* rose during the latter half of lifespan and division of these cells, but eventually declined over time in their descendants (Fig. 6). This dynamical phenomenon of division-order perturbation was also found in E2 and D1 (data not shown). For example, in D lineage, D1 exhibited a low positional variation during its lifespan until the occurrence of order-changed cell divisions AB16, E2 and D1 (Fig. 6a, Table 2); this induced variation decreased momentarily and went up again when another order-changed cell divisions D2, MS8 and P4 proceed, and then continue to recover.

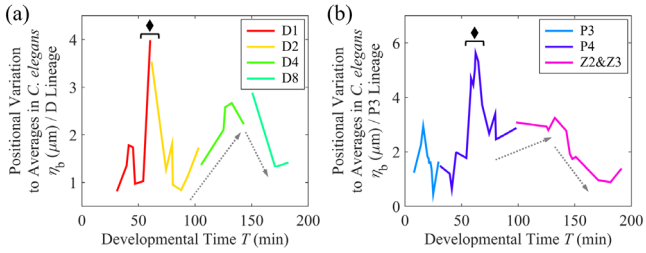

Fig. 6. Cellular positional variation to the averages of *C. elegans* embryos, according to (2). (a) D1, D2, D4 and D8 cells; (b) P3, P4 and Z2&Z3 cells; occurrence timing around AB16, E2 and D1 divisions is indicated with black diamond.

Even though the change of division order indeed enlarged the positional variation in specific influenced cells between *C. elegans* and *C. briggsae*, this effect could be rescued. As these cells are produced after the turning point, which is assumed to be initiation of the down regulation on global positional variation, it's plausible that this underlying mechanism gives rise to the spatial robustness against noise or perturbation raised by the variable cell division orders since gastrulation onset. Before that, this fail-safe "machine" may be not activated or dominant, so that the division orders are always controlled to be conserved and accurate, contributing to the stability of developmental procedures [8-10, 45]. Last but not least, the observation of variable cell division order between AB16 and E2 is in line with the experimental facts that, the AB blastomere is not necessary for the gastrulating movements of E cells [50].

IV. Local Difference between Species

In addition to division-order change between cell groups, the local difference of cell division timing between sister cells or neighboring cells may also have effect on their progenies' positions. Asynchrony of division between sister cells (hereafter referred to as ADS) has been proposed and systematically analyzed for each cell during *C. elegans* embryogenesis from 4- to 350-cell stage [22]. For any cell with at least two following rounds of division, its ADS was quantified by the difference of cell cycles between its daughters. ADS exists in a great number of cells, which was found to be regulated by genes involved with early maternal factor, signaling transduction (e.g. Wnt and Notch), transcription, chromatin modification, etc. Apart from cell-fate asymmetry, ADS is also assumed to organize the formation of a specific cell-arrangement pattern, by mechanical coordination similar to that before ~26-cell stage [8-10]. RNA interference on genes could not only severely perturb the ADS patterns in wild-type embryo, but also disturb the division timing and migration trajectory of many cells at the same time, leading to lethality in embryo and loss of high-confidence comparability.

To overcome the pleiotropic phenotypes and interconnected defects caused by mutation (e.g. division orientation, division timing, cell position), here we investigated the net effect as well as spatial function of ADS by comparing embryos of *C. elegans* and *C. briggsae*, which can both normally develop and hatch. Considering that the temporal resolution was 1.41 or 1.54 min/frame in experiment and the threshold of ADS classification was set to be 5 minutes before [22], here we searched all the cells and selected the ones with average ADS shorter than 2 minutes in one species but longer than 6 minutes in another, ensuring their substantial difference no less than trebling. Consequently, no additional ADS cell was found in *C. elegans* compared to *C. briggsae*. On the contrary, a total of four cells with extra ADS in *C. briggsae* were filtered under this arbitrary criterion (Fig. 7a), namely ABplappp, ABprappp, Eal and Ear. Eal and Ear are sisters, while their cousins Epl and Epr have remarkable ADS in both *C. elegans* and *C. briggsae* (Fig. 3). Interestingly, the sisters of ABplappp and ABprappp exhibit no asynchrony in their daughters' divisions in both species, although these two cell pairs are produced by the same mothers respectively. Therefore, these two pairs of lineal cells (ABplappa and ABplappp, ABprappa and ABprappp) could be good materials for comparative research on ADS as well as how it affects the local cell-arrangement pattern in *C. briggsae*, in consideration of their transcriptional and positional similarity.

Here, we investigated the relative locations of granddaughters of these 4 AB cells. To this end, the intersection angle θ was introduced to capture the feature of 4-cell structure formed by the granddaughters of each cell, respectively (Fig. 7b). In brief, each of ABplappa, ABplappp, ABprappa and ABprappp can be simplified and abbreviated as cell "X", which would divide into 2 daughters Xa and Xp, then divide again to produce Xaa, Xap, Xpa and Xpp. The vector orienting from Xaa to Xap is denoted by $\boldsymbol{\nu}_{\mathrm{Xaa}\rightarrow\mathrm{Xap}}$, while the one from Xpa to Xpp is denoted by $\boldsymbol{\nu}_{\mathrm{Xpa}\rightarrow\mathrm{Xpp}}$. θ is defined as the intersection angle of vectors $\boldsymbol{\nu}_{\mathrm{Xaa}\rightarrow\mathrm{Xap}}$ and $\boldsymbol{\nu}_{\mathrm{Xpa}\rightarrow\mathrm{Xpp}}$. The inspection timing was selected to be the first co-existence moment of AB256 cells. All the 4 AB cells in *C. elegans* as well as *C. briggsae* were taken into consideration and compared using θ (Fig. 7c). The cells without ADS in both species (i.e. ABplappa, ABprappa) had close degree of θ. However, the cells with extra ADS in *C. briggsae* (i.e. ABplappp, ABprappp) had significantly narrower intersection angle between $\boldsymbol{\nu}_{\mathrm{Xaa}\rightarrow\mathrm{Xap}}$ and $\boldsymbol{\nu}_{\mathrm{Xpa}\rightarrow\mathrm{Xpp}}$ (p-value < 0.1, Wilcoxon

rank-sum test). In a word, the asynchrony of division between sister cells functions in coordinating their 4 granddaughter cells' positions. In the cases of ABplappp and ABprappp, it seems to make the 4-cell structure formed by their granddaughters more parallel and less interlaced. This kind of spatial effect may further influence the contact relationship and area between cells, which could play a critical role in sensitive cell-cell communication [51].

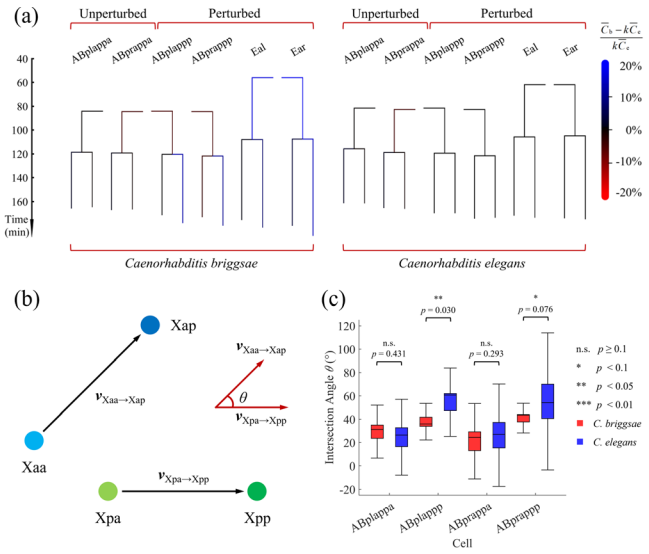

Fig. 7. Asynchrony of division between sister cells and its accompanying spatial effect. (a) Parts of cell lineage in *C. briggsae* (left) and *C. elegans* (right), including cells of ABplappa, ABprappa, ABplappp, ABprappp, Eal and Ear; (b) sketch map of relative locations among granddaughters from an original cell; (c) statistical comparison of intersection angle θ between *C. briggsae* and *C. elegans* in the 4 AB cells, using Wilcoxon rank-sum test.

V. Conclusion and Discussion

A. Method Introduction and Data Generation

Regarding embryogenesis and morphogenesis of metazoan animal, a fascinating question remains to be answered: how the cells interact with each other in space and time, and contribute to the precision and robustness of development in an embryo. In order to help solve this problem and push forward the systematic comparative study with abundant bioinformatics data, in this paper, we collected and provided complete and accurate cell-position data of 11 embryos respectively for nematodes *C. elegans* and *C. briggsae* from 4- to 350-cell stage, using 3D time-lapse *in vivo* imaging and automatic cell-tracking techniques. With the help of these two species, we introduced and demonstrated a computational pipeline to generate low-variation and standard dataset of comparable multicellular systems.

B. Investigating Spatio-Temporal Cellular Interactions in Embryonic Morphogenesis

Taking advantage of cell-position information of *C. elegans* and *C. briggsae*, we focused on the topic "spatio-temporal cellular interactions in embryonic morphogenesis". In short, we compared the orders between synchronous division events and found that the first dramatic chaos of division orders (i.e. AB16, E2, D1) appeared to occur around the robust onset of maternal-zygotic transition and gastrulation, which is also the turning point of global positional variation within *C. elegans* as well as between *C. elegans* and *C. briggsae*. Another two sets of later division orders around D2 and P4 divisions were found to be perturbed when development proceeds, along with fluctuating cellular positional variation which increased at first and then gradually declined, indicating a global down regulation on cellular positional variation shared in both species. Additionally, a previously reported phenomenon called asynchrony of division between sister cells (ADS) was investigated as a special case of local spatio-temporal cellular interactions, which exhibited a functional spatial effect in positioning the newborn cells and is worth of further exploration by mechanical simulation [8-10, 13-17, 52, 53].

C. Potential Application of the Method and Data

TABLE III. Perturbation on Cell Cycle

Lineage	Cell Name	Relative Deviation V (%) [P]
AB	ABplaa	10.0
	ABplap	11.1
	ABprap	10.8
	ABarppa	11.9
	ABarppp	11.1
	ABplapppp	14.6
	ABprapppp	12.6
	ABprpappa	-12.5
	ABprppapp	-10.1
MS	MSapa	18.6
	MSapp	14.7
	MSppa	16.2
	MSppp	16.0
E	Ea	-12.6
	Ep	-11.2
	Eal	18.5
	Ear	20.2
	Epl	14.0
	Epr	15.4
	Earp	16.1
	Epra	10.8
	Eprp	11.4
C	Ca	-12.0
	Cp	-13.3
	Cap	-10.6
	Cpap	11.4
	Cppp	10.4
D	D	-18.2

P. list of cells with relative deviation V larger than 10%.

With 4D cell-position data of *C. elegans* and *C. briggsae*, we selected a few special problems for developmental biology research. Note that the dataset of these two comparative systems can be extensively used for other fascinating biological topics, such as division orientation, cell-cell contact, communication and coordination. In addition to division-order chaos between cell groups, the drastic changes of cell cycle between *C. elegans* and *C. briggsae* were also found in an amount of specific cells (Table 3), possibly leading to other kinds of substantial local difference between these two species, which needs to be further validated. These cross-species materials are worth of mining deeply for understanding how developmental programs across species are evolved and optimized during evolution [38, 54]. The quantitative and analytic methods mentioned in this work can be applied onto other species (e.g. rotifer, gastrotrich) as well as multicellular systems like the genetically or mechanically perturbed embryos, and eutelic tissues and organs [2, 11, 25].

VI. Data Availability

The computation in this work was performed on Matlab. All the 4D raw images, quantitative data of the 22 embryos studied and other detailed information in this paper are public and available upon reasonable request.

Author Contributions

G. Guan, Z. Zhao, C. Tang conceived and coordinated the study; G. Guan performed computation, analyzed the data, and wrote the manuscript; M. K. Wong, L. Y. Chan, V. W. S. Ho, X. An performed embryo curation, imaging and editing; Z. Zhao, C. Tang provided theoretical instructions; Z. Zhao provided reagents and experimental methods for the project.

Acknowledgment

This work was supported by the National Natural Science Foundation of China (12090053, 32088101), the Hong Kong Research Grants Council (HKBU12100118, HKBU12100917, HKBU12123716) and the HKBU Interdisciplinary Research Cluster Fund. Some strains were provided by the *C. elegans* Genetic Center (CGC), which is funded by National Institutes of Health, Office of Research Infrastructure Programs, Grant P40 OD010440. The analysis was partly conducted on the High-Performance Computing Platform of the Center for Life Sciences at Peking University.

References

[1] J. E. Sulston, E. Schierenberg, J. G. White and J. N. Thomson, "The embryonic cell lineage of the nematode *Caenorhabditis elegans*," Developmental Biology, vol. 100, Nov. 1983, pp. 64-119, doi:10.1016/0012-1606(83)90201-4.

[2] G. Guan, M. K. Wong, V. W. S. Ho, X. An, L. Y. Chan, et al., "System-level quantification and phenotyping of early embryonic morphogenesis of *Caenorhabditis elegans*," bioRxiv (preprint, unpublished), Sept. 2019, 776062, doi:10.1101/776062.

[3] C. C. Mello, B. W. Draper and J. R. Priess, "The maternal genes *apx-1* and *glp-1* and establishment of dorsal-ventral polarity in the early *C. elegans* embryo," Cell, vol. 77, Apr. 1994, pp. 95-106, doi:10.1016/0092-8674(94)90238-0.

[4] S. E. Mango, C. J. Thorpe, P. R. Martin, S. H. Chamberlain and B. Bowerman, "Two maternal genes, *apx-1* and *pie-1*, are required to distinguish the fates of equivalent blastomeres in the early *Caenorhabditis elegans* embryo," Development, vol. 120, Aug. 1994, pp. 2305-2315, https://dev.biologists.org/content/develop/120/8/2305.

[5] L. Chen, V. W. S. Ho, M. K. Wong, X. Huang, L. Y. Chan, et al., "Establishment of signaling interactions with cellular resolution for every cell cycle of embryogenesis," Genetics, vol. 209, May 2018, pp. 37-49, doi:10.1534/genetics.118.300820.

[6] O. Bossinger and E. Schierenberg, "Cell-cell communication in nematode embryos: differences between *Cephalobus spec.* and *Caenorhabditis elegans*," Development Genes and Evolution, vol. 206, Jun. 1996, pp. 25-34, doi:10.1007/s004270050027.

[7] E. Schierenberg, "Embryological variation during nematode development (January 02, 2006)," WormBook, ed. The *C. elegans* Research Community, WormBook, doi:10.1895/wormbook.1.55.1.

[8] B. Tian, G. Guan, L. H. Tang and C. Tang, "Why and how the nematode's early embryogenesis can be precise and robust: a mechanical perspective," Physical Biology, vol. 17, Feb. 2020, 026001, doi:10.1088/1478-3975/ab6356.

[9] R. Fickentscher, P. Struntz and M. Weiss, "Setting the clock for fail-safe early embryogenesis," Physical Review Letters, vol. 117, Oct. 2016, 188101, doi:10.1103/PhysRevLett.117.188101.

[10] X. Kuang, G. Guan, M. K. Wong, L. Y. Chan, Z. Zhao, et al., "Computable early *C. elegans* embryo with a data-driven phase field model," bioRxiv (preprint, unpublished), Dec. 2020, 422560, doi:10.1101/2020.12.13.422560.

[11] H. J. V. Cleave, "Eutely or cell constancy in its relation to body size," The Quarterly Review of Biology, vol. 7, Mar. 1932, pp. 59-67, doi:10.1086/394396.

[12] A. K. Corsi, B. Wightman and M. Chalfie, "A transparent window into biology: a primer on *Caenorhabditis elegans*," Genetics, vol. 200, Jun. 2015, pp. 387-407, doi:10.1534/genetics.115.176099.

[13] R. Fickentscher, P. Struntz and M. Weiss, "Mechanical cues in the early embryogenesis of *Caenorhabditis elegans*," Biophysical Journal, vol. 105, Oct. 2013, pp. 1805-1811, doi:10.1016/j.bpj.2013.09.005.

[14] R. Fickentscher, S. W. Krauss and M. Weiss, "Anti-correlation of cell volumes and cell-cycle times during the embryogenesis of a simple model organism," New Journal of Physics, vol. 20, Nov. 2018, 113001, doi:10.1088/1367-2630/aaea91.

[15] A. Kajita, M. Yamamura and Y. Kohara, "Physical modeling of the cellular arrangement in *C. elegans* early embryo: effect of rounding and stiffening of the cells," Genome Informatics, vol. 13, 2002, pp. 224-232, doi:10.11234/gi1990.13.224.

[16] A. Kajita, M. Yamamura and Y. Kohara, "Computer simulation of the cellular arrangement using physical model in early cleavage of the nematode *Caenorhabditis elegans*," Bioinformatics, vol. 19, Apr. 2003, pp. 704-716, doi:10.1093/bioinformatics/btg069.

[17] K. Yamamoto and A. Kimura, "An asymmetric attraction model for the diversity and robustness of cell arrangement in nematodes," Development, vol. 144, Dec. 2017, pp. 4437-4449, doi:10.1242/dev.154609.

[18] J. Nance, E. M. Munro and J. R. Priess, "*C. elegans* PAR-3 and PAR-6 are required for apicobasal asymmetries associated with cell adhesion and gastrulation," Development, vol. 130, Nov. 2003, pp. 5339-5350, doi:10.1242/dev.00735.

[19] J. Y. Lee, D. J. Marston, T. Walston, J. Hardin, A. Halberstadt and B. Goldstein, "Wnt/Frizzled signaling controls *C. elegans* gastrulation by activating actomyosin contractility," Current Biology, vol. 16, Oct. 2006, pp. 1986-1997, doi:10.1016/j.cub.2006.08.090.

[20] K. Sugioka and B Bowerman, "Combinatorial contact cues specify cell division orientation by directing cortical myosin flows," Developmental Cell, vol. 46, Aug. 2018, pp. 257-270, doi:10.1016/j.devcel.2018.06.020.

[21] C. R. Hsu, R. Xiong and K. Sugioka, "In vitro reconstitution of spatial cell contact patterns with isolated *Caenorhabditis elegans* embryo blastomeres and adhesive polystyrene beads," Journal of Visualized Experiments, vol. 153, Nov. 2019, e60422, doi:10.3791/60422.

[22] V. W. S. Ho, M. K. Wong, X. An, D. Guan, J. Shao, et al., "Systems-level quantification of division timing reveals a common genetic architecture controlling asynchrony and fate asymmetry," Molecular Systems Biology, vol. 11, Jun. 2015, 814, doi:10.15252/msb.20145857.

[23] H. Hutter and R Schnabel, "*glp-1* and inductions establishing embryonic axes in *C. elegans*," Development, vol. 120, Jul. 1994, pp. 2051-2064, https://dev.biologists.org/content/develop/120/7/2051.

[24] E. Schierenberg and B. Junkersdorf, "The role of eggshell and underlying vitelline membrane for normal pattern formation in the early *C. elegans* embryo," Roux's Archives of Developmental Biology, vol. 202, Dec. 1992, pp. 10-16, doi:10.1007/BF00364592.

[25] R. Jelier, A. Kruger, J. Swoger, T. Zimmermann and B. Lehner, "Compensatory cell movements confer robustness to mechanical deformation during embryonic development," Cell Systems, vol. 3, Aug. 2016, pp. 160-171, doi:10.1016/j.cels.2016.07.005.

[26] L. Zou, S. Sriswasdi, B. Ross, P. V. Missiuro, J. Liu and H. Ge, "Systematic analysis of pleiotropy in *C. elegans* early embryogenesis," PLoS Computational Biology, vol. 4, Feb. 2008, e1000003, doi:10.1371/journal.pcbi.1000003.

[27] E. Schierenberg, "Early development of nematode embryos: differences and similarities," Nematology, vol. 2, Jan. 2000, pp. 57-64, doi:10.1163/156854100508890.

[28] W. Houthoofd and G. Borgonie, "The embryonic cell lineage of the nematode *Halicephalobus gingivalis* (Nematoda: Cephalobina: Panagrolaimoidea)," Nematology, vol. 9, Jan. 2007, pp. 573-584, doi:10.1163/156854107781487288.

[29] J. Schulze and E. Schierenberg, "Evolution of embryonic development in nematodes," EvoDevo, vol. 2, Sept. 2011, 18, doi:10.1186/2041-9139-2-18.

[30] J. Schulze, W. Houthoofd, J. Uenk, S. Vangestel and E. Schierenberg, "*Plectus* - a stepping stone in embryonic cell lineage evolution of nematodes," EvoDevo, vol. 3, Jul. 2012, 13, doi:10.1186/2041-9139-3-13.

[31] J. Schulze and E. Schierenberg, "Cellular pattern formation, establishment of polarity and segregation of colored cytoplasm in embryos of the nematode *Romanomermis culicivorax*," Developmental Biology, vol. 315, Jan. 2008, pp. 426-436, doi:10.1016/j.ydbio.2007.12.043.

[32] J. Schulze and E. Schierenberg, "Embryogenesis of *Romanomermis culicivorax*: an alternative way to construct a nematode," Developmental Biology, vol. 334, Oct. 2009, pp. 10-21, doi:10.1016/j.ydbio.2009.06.009.

[33] D. A. Voronov and Y. V. Panchin, "Cell lineage in marine nematode *Enoplus brevis*," Development, vol. 125, Jan. 1998, pp. 143-150, https://dev.biologists.org/content/develop/125/1/143.

[34] W. Houthoofd, M. Willems, K. Jacobsen, A. Coomans and G. Borgonie, "The embryonic cell lineage of the nematode *Rhabditophanes* sp.," International Journal of Developmental Biology, vol. 52, Aug. 2008, pp. 963-967, doi:10.1387/ijdb.072404wh.

[35] W. Houthoofd, M. Willems, S. Vangestel, C. Mertens, W. Bert and G. Borgonie, "Different roads to form the same gut in nematodes," Evolution & Development, vol. 8, Jun. 2006, pp. 362-369, doi:10.1111/j.1525-142X.2006.00108.x.

[36] S. E. Baird and W. C. Yen, "Reproductive isolation in *Caenorhabditis*: terminal phenotypes of hybrid embryos," Evolution & Development, vol. 2, Dec. 2001, pp. 9-15, doi:10.1046/j.1525-142x.2000.00031.x.

[37] Z. Zhao, T. J. Boyle, Z. Bao, J. I. Murray, B. Mericle and R. H. Waterston, "Comparative analysis of embryonic cell lineage between *Caenorhabditis briggsae* and *Caenorhabditis elegans*," Developmental Biology, vol. 314, Feb. 2008, pp. 93-99, doi:10.1016/j.ydbio.2007.11.015.

[38] N. Memar, S. Schiemann, C. Henniga, D. Findeis, B. Conradt and R. Schnabel, "Twenty million years of evolution: The embryogenesis of four *Caenorhabditis* species are indistinguishable despite extensive genome divergence," Developmental Biology, vol. 447, Mar. 2019, pp. 182-199, doi:10.1016/j.ydbio.2018.12.022.

[39] D. Rudel and J. Kimble, "Conservation of *glp-1* regulation and function in nematodes," Genetics, vol. 157, Feb. 2001, pp. 639-654, https://www.genetics.org/content/genetics/157/2/639.

[40] D. Rudel and J. Kimble, "Evolution of discrete Notch-like receptors from a distant gene duplication in *Caenorhabditis*," Evolution & Development, vol. 4, Sept. 2002, pp. 319-333, doi:10.1046/j.1525-142X.2002.02027.x.

[41] L. D. Stein, Z. Bao, D. Blasiar, T. Blumenthal, M. R. Brent, et al., "The genome sequence of *Caenorhabditis briggsae*: a platform for comparative genomics," PLoS Biology, vol. 1, Nov. 2003, pp. 166-192, doi:10.1371/journal.pbio.0000045.

[42] Z. Bao, J. I. Murray, T. Boyle, S. L. O. Ooi, M. J. Sandel and R. H. Waterston, "Automated cell lineage tracing in *Caenorhabditis elegans*," Proceedings of the National Academy of Sciences of the United States of America, vol. 103, Feb. 2006, pp. 2707-2712, doi:10.1073/pnas.0511111103.

[43] T. J. Boyle, Z. Bao, J. I. Murray, C. L. Araya and R. H. Waterston, "AceTree: a tool for visual analysis of *Caenorhabditis elegans* embryogenesis," BMC Bioinformatics, vol. 7, Jun. 2006, 275, doi:10.1186/1471-2105-7-275.

[44] J. I. Murray, Z. Bao, T. J. Boyle and R. H. Waterston, "The lineaging of fluorescently labeled *Caenorhabditis elegans* embryos with StarryNite and AceTree," Nature Protocols, vol. 1, Nov. 2006, pp. 1468-1476, doi:10.1038/nprot.2006.222.

[45] X. Li, Z. Zhao, W. Xu, R. Fan, L. Xiao, et al., "Systems properties and spatiotemporal regulation of cell position variability during embryogenesis," Cell Reports, vol. 26, Jan. 2019, pp. 313-321. doi:10.1016/j.celrep.2018.12.052.

[46] J. I. Murray, T. J. Boyle, E. Preston, D. Vafeados, B. Mericle, et al., "Multidimensional regulation of gene expression in the *C. elegans* embryo," Genome Research, vol. 22, Jul. 2012, pp. 1282-1294, doi:10.1101/gr.131920.111.

[47] Z. Zhao, S. Flibotte, J. I. Murray, D. Blick, T. J. Boyle, et al., "New tools for investigating the comparative biology of *Caenorhabditis briggsae* and *C. elegans*," vol. 184, Mar. 2010, pp. 853-863, doi:10.1534/genetics.109.110270.

[48] J. Cao, G. Guan, V. W. S. Ho, M. K. Wong, L. Y. Chan, et al., "Establishment of a morphological atlas of the *Caenorhabditis elegans* embryo using deep-learning-based 4D segmentation," vol. 11, Dec. 2020, 6254, doi:10.1038/s41467-020-19863-x.

[49] M. K. Wong, D. Guan, K. H. C. Ng, V. W. S. Ho, X. An, et al., "Timing of tissue-specific cell division requires a differential onset of zygotic transcription during metazoan embryogenesis," Journal of Biological Chemistry, vol. 291, Jun. 2016, pp. 12501-12513, doi:10.1074/jbc.M115.705426.

[50] J. Nance, J. Y. Lee and B. Goldstein, "Gastrulation in *C. elegans* (September 26, 2005)," WormBook, ed. The *C. elegans* Research Community, WormBook, doi:10.1895/wormbook.1.23.1.

[51] O. Shaya, U. Binshtok, M. Hersch, D. Rivkin, S. Weinreb, et al., "Cell-cell contact area affects Notch signaling and Notch-dependent patterning," Developmental Cell, vol. 40, Mar. 2017, pp. 505-511, doi:10.1016/j.devcel.2017.02.009.

[52] G. Guan, L. H. Tang and C. Tang, "Reconstructing the multicellular structure of a developing metazoan embryo with repulsion-attraction model and cell-cell connection atlas *in vivo*," Journal of Physics: Conference Series, vol. 1592, May 2020, 012020, doi:10.1088/1742-6596/1592/1/012020.

[53] J. Miao, G. Guan and C. Tang, "Spontaneous cell internalization of a spatially-confined proliferating blastomere: A mechanical interpretation on worm gastrulation," arXiv (preprint, unpublished), May 2021, 2105.05795v1, https://arxiv.org/abs/2105.05795.

[54] G. Guan, M. K. Wong, Z. Zhao, L. H. Tang and C. Tang, "Speed and fate diversity tradeoff in nematode's early embryogenesis," arXiv (preprint, unpublished), Mar. 2021, 2007.05723v2, https://arxiv.org/abs/2007.05723.